Electronic Supplementary Information

Heterojunction construction by coordination bond between metal-organic frameworks and $CdIn_2S_4$ for improved photocatalytic performance

Haijun Hu[a], Xiaodong Sun*[a], Kailai Zhang[a], Yang Chen[a], Hui Li[b], Hongwei Huang[d], Yali Ma*[c], and Tianyi Ma*[b]

[a] *Institute of Clean Energy Chemistry, Key Laboratory for Green Synthesis and Preparative Chemistry of Advanced Materials, College of Chemistry, Liaoning University, Shenyang 110036, People's Republic of China*

[b] *School of Science, RMIT University, Melbourne, VIC 3000, Australia*

[c] *College of Chemical Engineering, Shenyang University of Chemical Technology, Shenyang 110142, P. R. China*

[d] *Beijing Key Laboratory of Materials Utilization of Nonmetallic Minerals and Solid Wastes, National Laboratory of Mineral Materials, School of Materials Science and Technology, China University of Geosciences, Beijing, 100083, China*

*Corresponding author.
E-mail address: sunxiaodong@lnu.edu.cn; tianyi.ma@rmit.edu.au; mayalichem@126.com

1. Characterization

SEM images were acquired using a Hitachi SU-8010 equipped with an EDS analyzer. TEM and HRTEM images were obtained on a JEM-2100 operating at 5 kV. XRD patterns were collected using a D8 Advance (Bruker) X-ray diffraction system with a Cu Kα radiation (λ = 0.15406 nm). XPS spectra were recorded by the Thermo Scientific ESCALAB 250Xi spectrometer equipped with a monochromatic Al Kα X-ray source (1486.6 eV). The UV-vis spectra were obtained by the Ultraviolet-visible diffuse reflectance spectroscopy (UV-vis DRS) with $BaSO_4$ as the reflectance standard (Shimadzu UV-2550). Thermogravimetric analysis (TGA, METTLER TOLEDO TGA/SDTA851) was performed to analyze the structure of NH_2-UiO-66/$CdIn_2S_4$ with a heating rate of 5 °C·min^{-1} under air atmosphere. The surface area of prepared samples was investigated by nitrogen adsorption-desorption measurements (QuantaAutosorb IQ). Fluorescence measurements were carried out with the RF-5301PC (Shimadzu, Japan) fluorescence spectrophotometer (excitation wavelength: 320 nm).

2. Photocatalytic hydrogen production properties

Photocatalytic experiments were carried out via a full glass automatic on-line trace gas analysis system (Labsolar-6A, Beijing Perfectlight Technology Co., Ltd.). The light source is the 300 W Xenon lamp (wavelength: 320-780 nm, PLS-SXE300/300UV, light intensity: 100 mW·cm^{-2}, Beijing Perfectlight Technology Co., Ltd.). Hydrogen was detected and quantitative analyzed by a GC7900 gas chromatography (Shanghai Tianmei Scientific Instrument Co.) with nitrogen as the carrier gas, and the detection interval was 30 min. The catalyst was placed in a custom-made quartz glass reactor,

and the reaction temperature was controlled at 5 °C by condensing water. 30 mg of catalyst was added into 90 mL of deionized water with 10 mL of lactic acid as sacrificial agent. Then 3% Pt was added as a co-catalyst by photo-deposition of H_2PtCl_6 solution. After that, the suspension was stirred in a 200 mL customized quartz reactor. Before each photocatalytic reaction, the system was vacuum-treated several times to remove the dissolved air. The whole reaction system was illuminated by the Xe light irradiation with a UV cut-off filter ($\lambda \geq 420$ nm). The vertical distance between the Xe lamp source and the quartz glass reactor is approximately 3 cm.

3. Photoelectrochemical characterization

The electrochemical measurement was carried out by the electrochemical workstation with the model of CHI 760. The test was carried out in a three-electrode system, in which the Pt sheet was used as the counter electrode, the Ag/AgCl electrode was used as the reference electrode, and the prepared powder sample was used as the working electrode. In addition, 0.2 M Na_2SO_4 was used as the electrolyte solution, and a xenon lamp equipped with a filter ($\lambda \geq 420$ nm) was used as the visible light source. 5 mg of catalyst sample and 20 μl of Nafion solution were dissolved in 1 mL of anhydrous ethanol solution, sonicated for 30 min to make them evenly mixed, and then scraped onto FTO glass (1 cm × 1 cm) to prepare the working electrode.

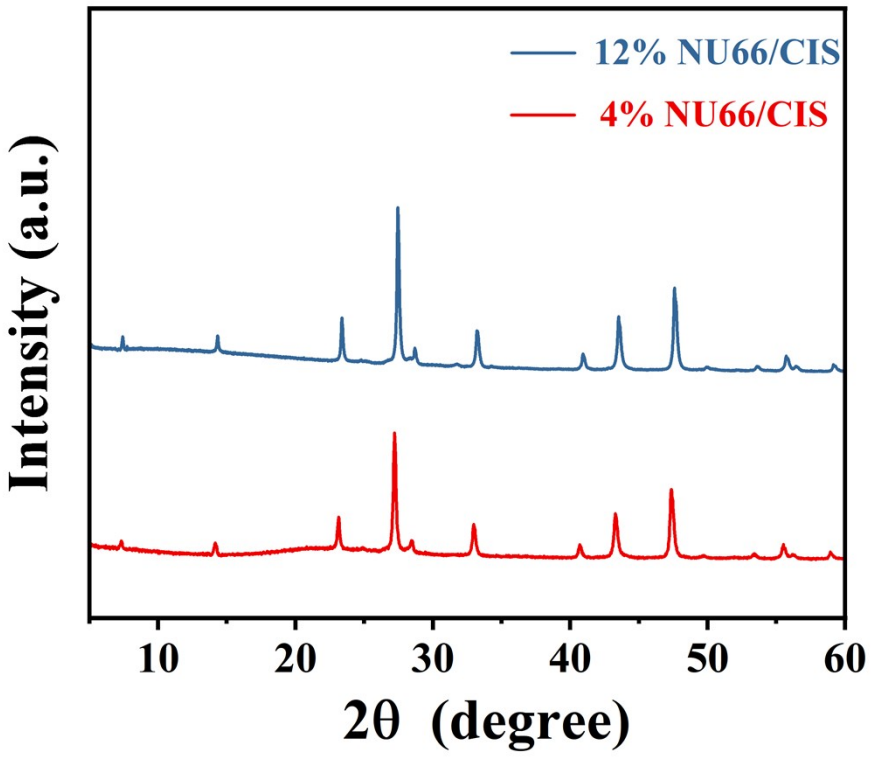

Fig. S1. The PXRD pattern of synthesized samples. As shown in Fig.S1, the coexistence of NU66 and CIS in the composites was also demonstrated by the PXRD tests of 4%NU66/CIS and 12%NU66/CIS, again proving the successful preparation of the catalysts.

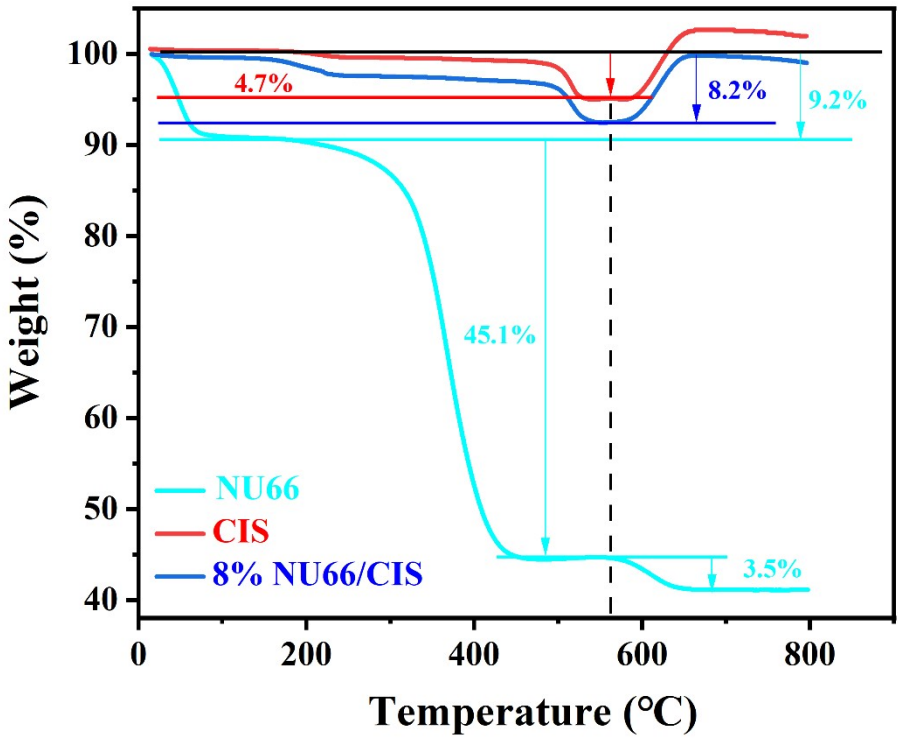

Fig. S2. The TGA patterns of the NU66, CIS and 8%NU66/CIS. On the basis of the thermogravimetric analysis (TGA) result, the masses of NU66, CIS and 8%NU66/CIS initially decrease with increasing temperature. When the temperature reaches about 560 °C, the mass loss of NU66/CIS is about 8.2 wt% between NU66 and CIS, demonstrating the the successful synthesis of NU66/CIS composite.

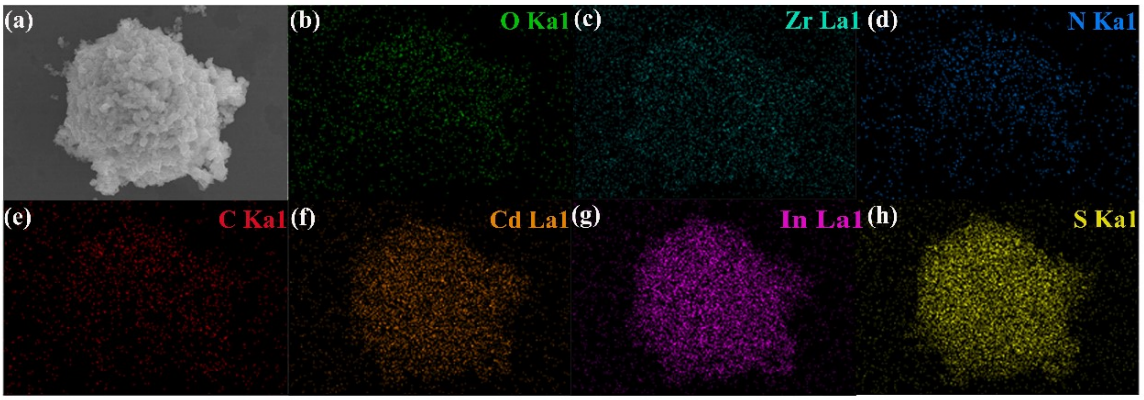

Fig. S3. The SEM-EDS mapping images of 8% NU66/CIS. Energy dispersive spectrometer (EDS) mapping tests were conducted to further confirm the construction of heterojunction structure. As shown in Fig.S3, seven elements O, Zr, N, C, Cd, In, S can be apparently seen in the mapping pictures, densely distributing in the composite. SEM-EDS mapping results demonstrate the successful formation of NU66/CIS composite again.

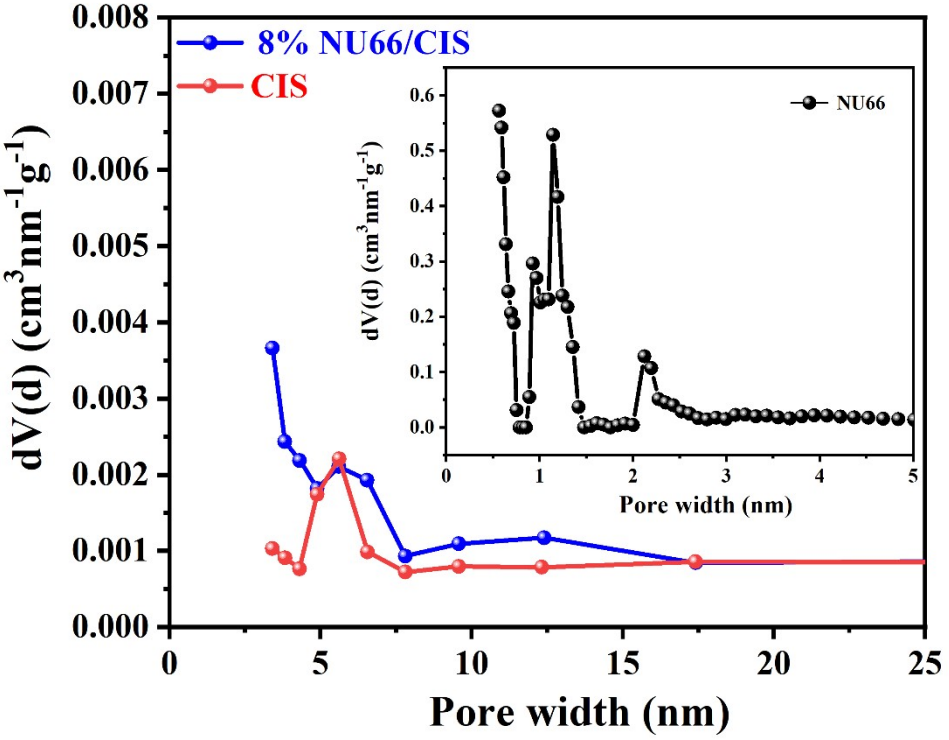

Fig. S4. The pore size distribution (adsorption branch) for NU66, CIS and 8% NU66/CIS. The pore size distribution (adsorption branch) for prepared photocatalysts are shown in Fig.S4, in which NU66 contains a large number of widely distributed micropores, and its pore specific surface area and pore volume are 864.5 $m^2 \cdot g^{-1}$ and 0.43 $cm^3 \cdot g^{-1}$, respectively.[1]

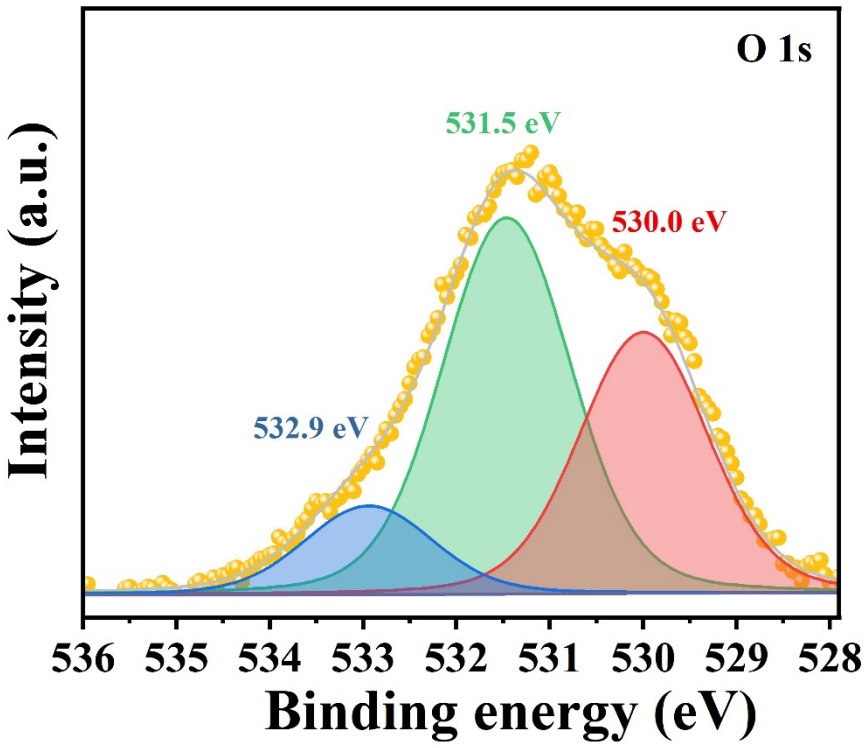

Fig. S5. The O 1s XPS spectra of 8%NU66/CIS composite. In Fig.S5, the O 1s spectrum of the 8%NU66/CIS sample can be split into three peaks at 530.0 eV, 531.5 eV and 532.9 eV, representing the Zr-O, C=O groups and surface-adsorbed -OH groups.[2]

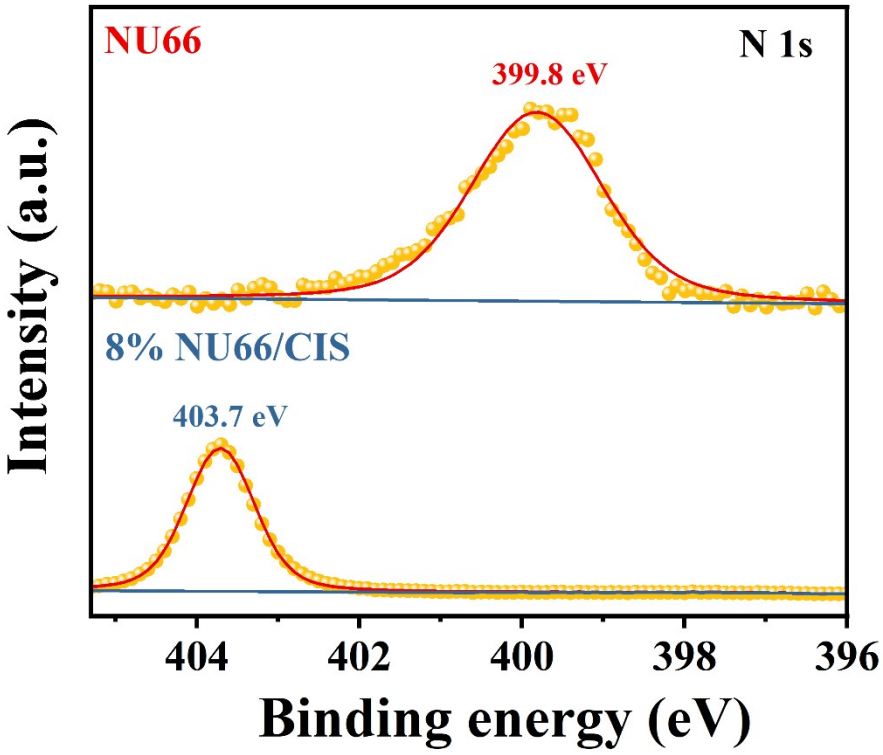

Fig. S6. The N 1s XPS spectra of pure NU66 and 8%NU66/CIS composite. As depicted in Fig.S6, the N 1 s spectrum of pure NU66 at 399.8 eV were related to -NH_2 groups, which were obviously shifted towards lower binding energies as compared to 8%NU66/CIS, demonstrating that the coordination between NU66 and CIS changed its chemical environment[3]. Thus, it was the amino groups that played a significant role in powerful interactions between NU66 and CIS, which was conducive to electron transport between two materials[4].

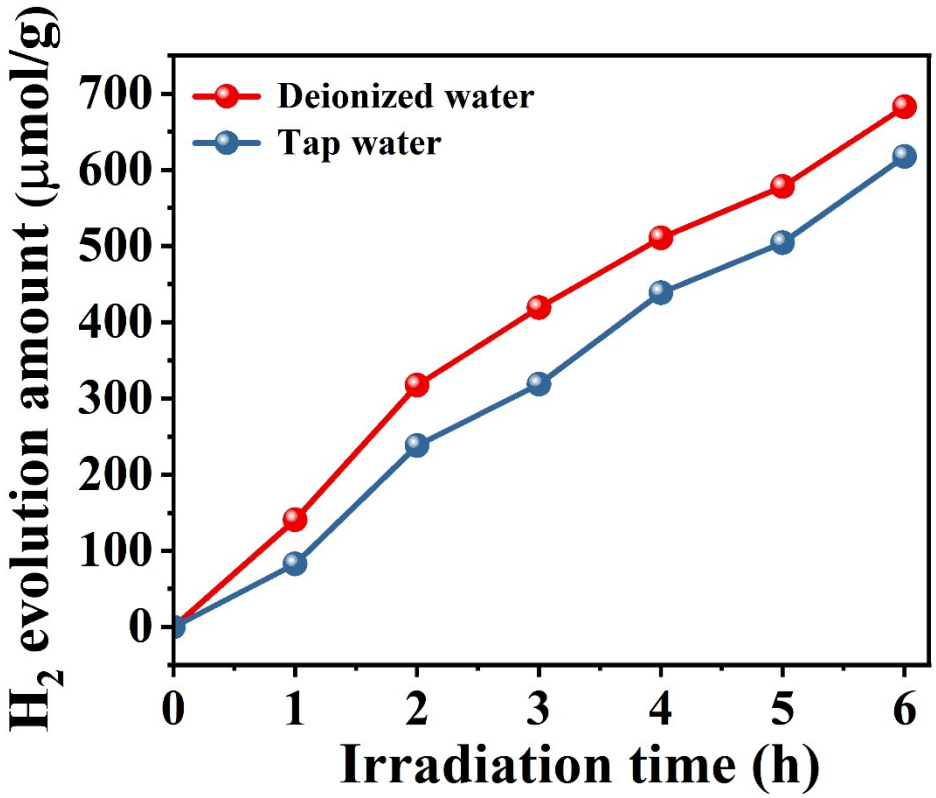

Fig. S7. Photocatalytic activity of 8%NU66/CIS in deionized water and tap water. As depicted in Fig.S7, 8%NU66/CIS shows relatively poor photocatalytic performance in tap water compared to that in deionized water due to the influence of impurities in tap water.

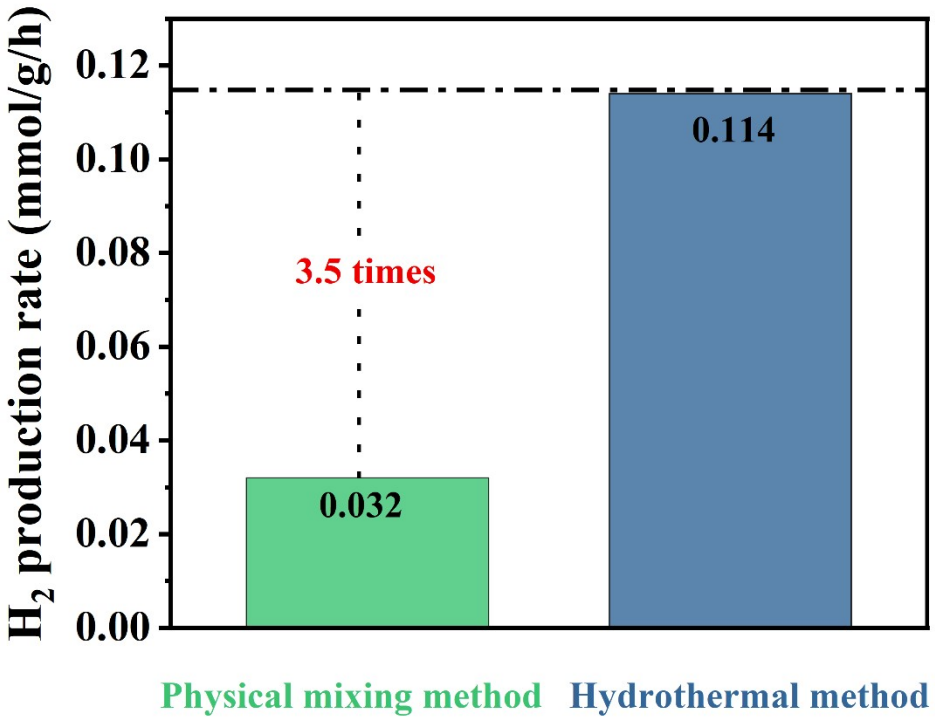

Fig. S8. Photocatalytic H_2 production rate of NU66/CIS via physical mixing or hydrothermal method. As shown in Fig.S8, the photocatalytic hydrogen production rate of 8%NU66/CIS was approximately 3.5 times that of two materials via physical mixing, because amino group induced NU66/CIS heterojunctions promoted the transfer of photogenerated charges.

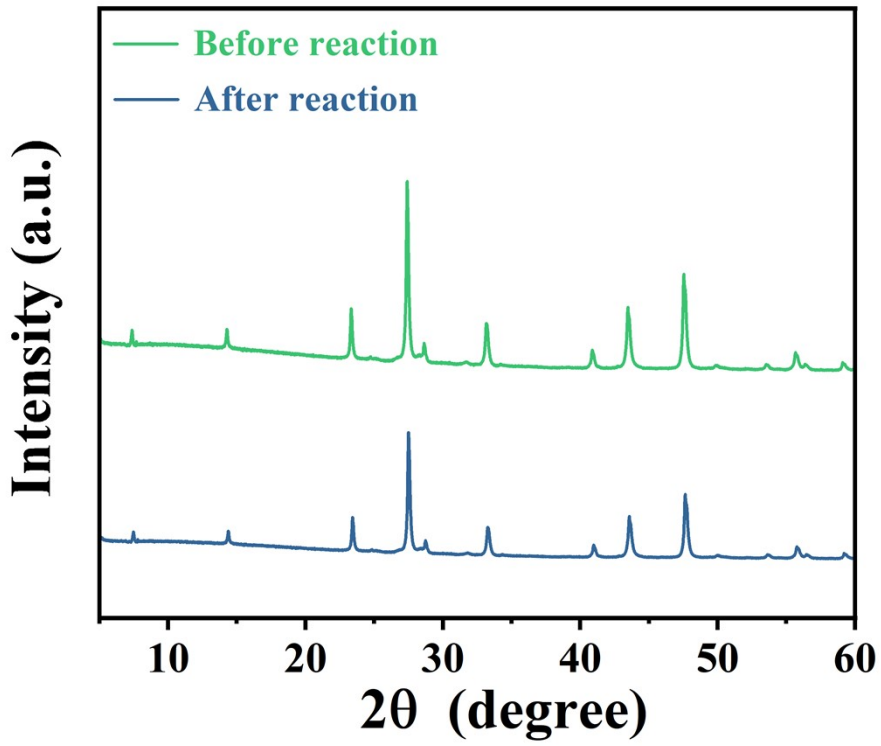

Fig. S9. The PXRD figure of 8%NU66/CIS before and after photocatalytic reaction. The PXRD test was carried out on NU66/CIS composite before and after photocatalytic reaction. It can be seen from Fig.S9 that the peak position and intensity of NU66/CIS almost did not change compared with those before the reaction, further proving the recyclability of the material.

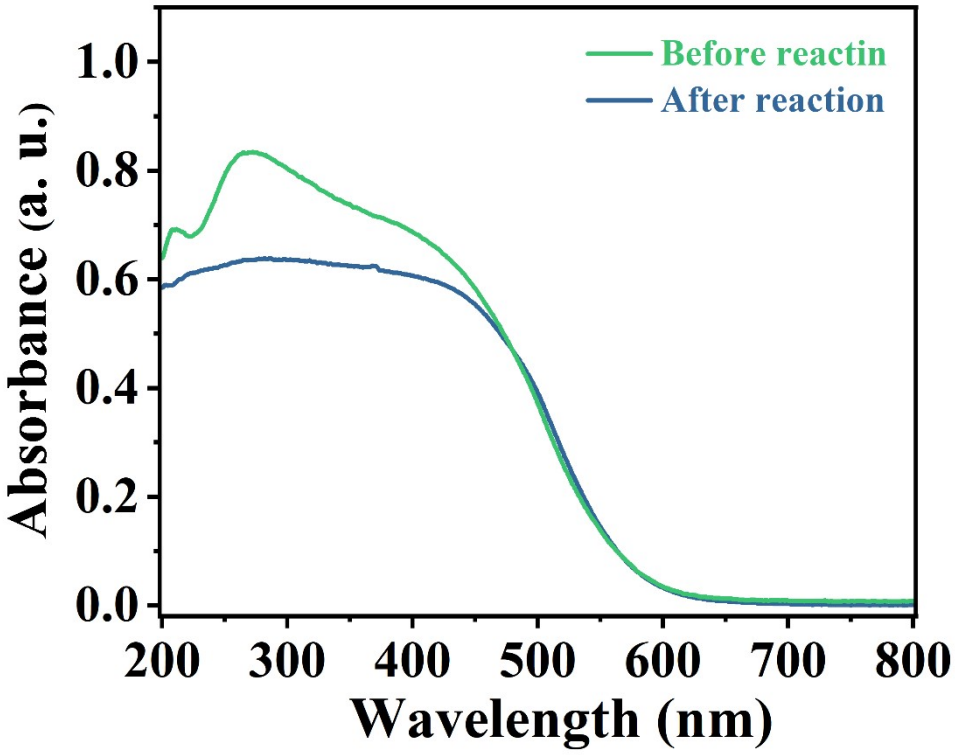

Fig. S10. The UV-Vis diffuse reflectance spectra of 8%NU66/CIS before and after photocatalytic reaction. As shown in Fig.S10, the light absorption range of the catalyst after photocatalytic reaction remains almost unchanged compared to that before the reaction, which further proves the durability of 8%NU66/CIS.

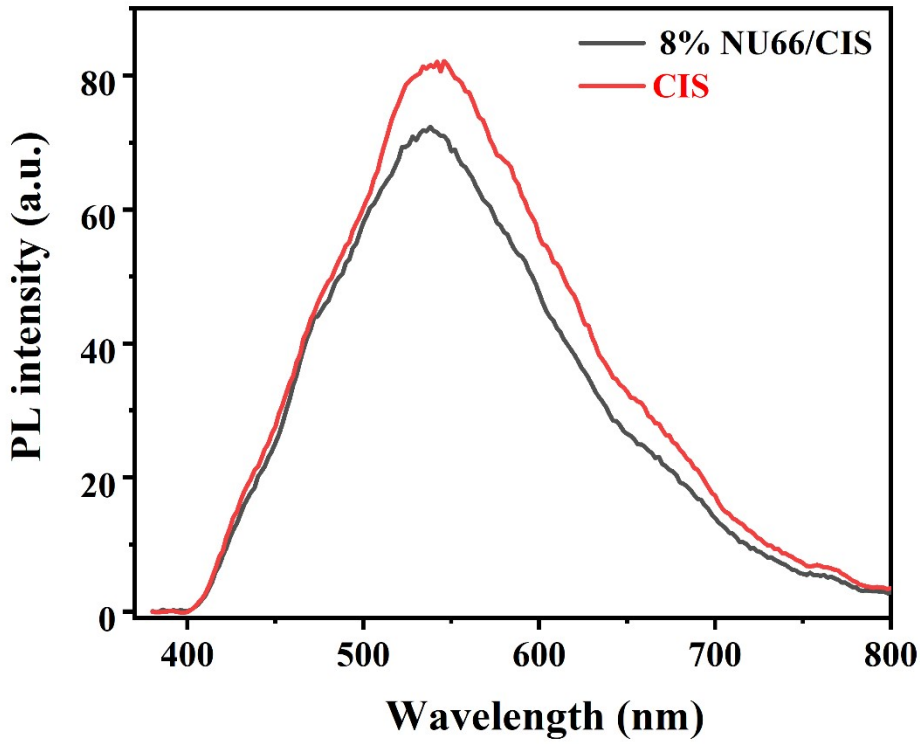

Fig. S11. The PL spectrum of CIS and 8%NU66/CIS. As shown in Fig.S11, the photoluminescence (PL) spectra was used to further investigate the carrier recombination properties of the photocatalysts. Obviously, the photoluminescence intensity of 8%NU66/CIS was weaker than that of CIS, because the construction of the heterojunction reduces the recombination rate of photogenerated electron-hole pairs.[5] The analysis results of PL spectra can be well matched with the photocatalytic performance.

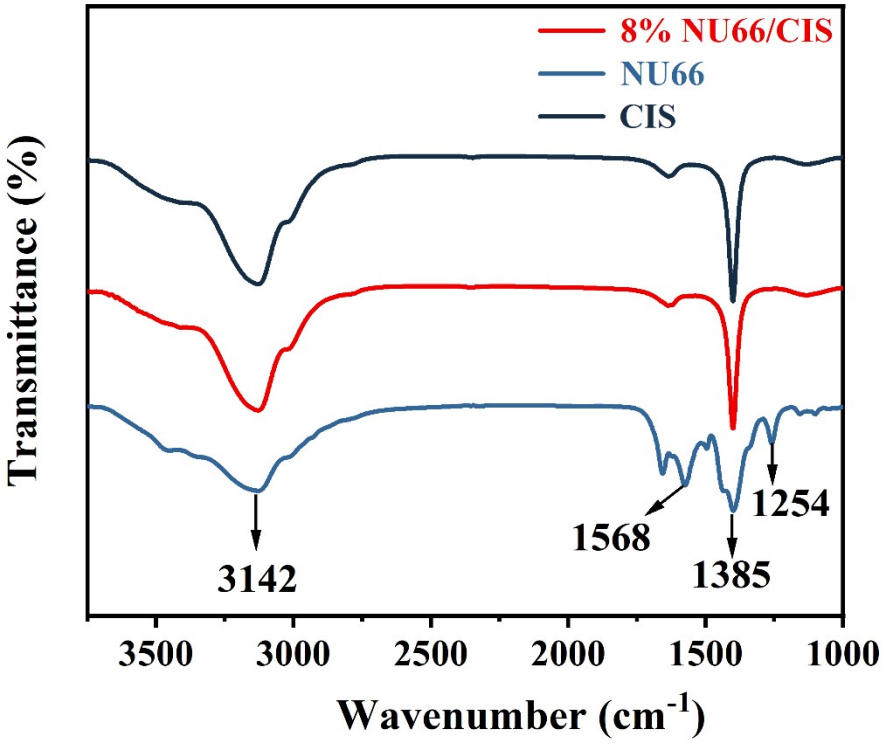

Fig. S12. Fourier-transform infrared (FT-IR) spectra of NU66, CIS and 8% NU66/CIS. As shown in Fig.S12, the major and sharp bands located at 1568 cm^{-1} and 1385 cm^{-1} were resulted from COO asymmetric and symmetric stretching vibrations of terephthalate groups, respectively. The broad band at about 3142 cm^{-1} was due to the stretching vibrations of both NH_2 groups of 2-aminoterephtalate ligand and surface adsorbed H_2O molecules. In addition，the band located at 1254 cm^{-1} could be assigned to the C-N stretching vibration of the ligand.[6]

Table1. The BET surface area of NU66, CIS and 8%NU66/CIS

Catalyst	BET surface area ($m^2 \cdot g^{-1}$)
CIS	16.4
8%NU66/CIS	21.7
NU66	855.3

Table2. The lifetime of CIS and 8%NU66/CIS in time-resolved PL test.

Catalyst	τ_1 (ns)	B_1	τ_2 (ns)	B_2	τ_{av} (ns)
CIS	1.742	204.255	6.924	99.482	5.159
8%NU66/CIS	0.628	264.210	4.917	59.799	3.369

References

1 Y. Wang, Q. Yang, F. Yi, R. Lu, Y. Chen, C. Liu, X. Li, C. Wang, H. Yan, *ACS Appl. Mater. Interfaces*, 2021, **13,** 29916-29925.

2 Z. Yang, X. Tong, J. Feng, S. He, M. Fu, X. Niu, T. Zhang, H. Liang, A. Ding, X. Feng, *Chemosphere*, 2019, **220,** 98-106.

3 M. S. Hosseini, A. Abbasi, M. Masteri-Farahani, *J. Hazard. Mater.*, 2022, **425,** 127975.

4 X. Wei, C. C. Wang, Y. Li, P. Wang, Q. Wei, *Chemosphere*, 2021, **280,** 130734.

5 J. Gao, F. Zhang, H. Xue, L. Zhang, Y. Peng, X. Li, Y. Gao, N. Li, G. Lei, *Appl. Catal., B*, 2021, **281,** 119509.

6 S. Subudhi, G. Swain, S. P. Tripathy, K. Parida, *Inorg. Chem.*, 2020, **59,** 9824-9837.